Chemical Physics Letters 746 (2020) 137298

Contents lists available at ScienceDirect

Chemical Physics Letters

journal homepage: www.elsevier.com/locate/cplett

Research paper

Water enhanced mechanism for CO_2 – Methanol conversion

Rachid Hadjadj[a], Imre G. Csizmadia[a,c], Péter Mizsey[a], Svend Knak Jensen[d], Béla Viskolcz[a], Béla Fiser[a,b,*]

[a] Institute of Chemistry, University of Miskolc, 3515 Miskolc-Egyetemváros, Hungary
[b] Ferenc Rákóczi II. Transcarpathian Hungarian Institute, 90200 Beregszász, Transcarpathia, Ukraine
[c] Department of Chemistry, University of Toronto, Toronto, M5S 1A1 Ontario, Canada
[d] Department of Chemistry, Langelandsgade 140, Aarhus University, DK-8000 Aarhus C, Denmark

HIGHLIGHTS

- CO_2–CH_3OH conversion in aqueous phase has been envisaged: (CO_2 + $3H_2$ + H_2O + H_3O^+).
- The reaction has been investigated by using the high level W1U composite method.
- Hydrogenations are the least favourable steps in the reaction.
- The energy storage efficiency of the studied mechanism is 27.1%.
- Catalysts can be designed to decrease the energy barrier and increase efficiency.

ARTICLE INFO

Keywords:
Carbon dioxide hydrogenation
Climate change
Computational study
Energy storage

ABSTRACT

Carbon dioxide can be converted into fine chemicals such as methanol and thus, the produced renewable energy can be stored in chemical bonds through reductions. To achieve this, a water enhanced mechanism of CO_2 hydrogenation leading to methanol has been designed by applying 1:3 (CO_2 + $3H_2$) extended with a water molecule and a hydronium. The thermodynamic properties of the intermediate species and transition states have been calculated by using the W1U composite method. The energy efficiency of the studied mechanism is 27.1%. By understanding the mechanism, special purpose catalysts can be designed to accelerate carbon dioxide conversion.

1. Introduction

It is widely known that carbon dioxide (CO_2) release in nature has a detrimental effect, and research in environmental protection is a challenge nowadays [1]. Since the industrial revolution, CO_2 emissions did not stop increasing [2], which could be one of the possible factors behind global warming and the acidification of the oceans [3]. These adverse processes should be prevented by either inhibiting the release or developing large scale carbon dioxide capturing procedures. Most of the solutions proposed till now are mainly Carbon Capture and Storage (CCS) methods, which are not definitive solutions to eradicate the excess of CO_2 from the atmosphere [4]. Some ocean scientists think that ocean storage of CO_2 might be a good idea. In this case, the gas would be injected and trapped into the deep ocean [5], but will it stay there forever? Will it not be able to diffuse? From a chemical point of view, the best solution would be the total transformation of carbon dioxide into added value products [6], and in this way the produced renewable energy can also be stored [7]. Renewable energy production is not stable, and highly depends on the weather and other factors, and the energy consumption fluctuates as well, which means that the energy storage is unavoidable [8]. The common solution to both of these problems is to use renewable energy to convert carbon dioxide chemically into different molecules such as formic acid, formaldehyde, methanol or methane for the sake of energy storage [9]. These molecules can be used not only for the storage and production of energy, but to produce other chemicals in a renewable basis [10]. Energy will be stored in chemical bonds by recycling of carbon dioxide via hydrogenative reductions, and the hydrogen would be obtained from electrolysis using renewable electrical energy [11], which ideally will contribute to the decrease of CO_2 emission [12]. Carbon dioxide can be collected from several sources such as the industrial or biochemical processes [13], and the hydrogen has also many possible sources such

* Corresponding author.
E-mail address: kemfiser@uni-miskolc.hu (B. Fiser).

https://doi.org/10.1016/j.cplett.2020.137298
Received 11 January 2020; Received in revised form 18 February 2020; Accepted 1 March 2020
Available online 02 March 2020

as the electrolysis of water or steam reforming of natural gas [14]. Methanol and methane are the most attractive compounds to achieve from CO_2, due to their high energy content and their ability to be re-introduced into other chemical processes as feedstock to produce more advanced chemicals [15]. Between the different methanol production processes, CO_2 can be reduced directly, or introduced first in a reverse gas shift reactor (RWGS) as a fraction of synthesis gas [16]. In the last decades the CO_2 hydrogenation to methanol has been a widespread subject of interest, large variety of solid catalysts have been designed and tested [17], nevertheless the reduction mechanism is still a debated subject and new processes are proposed [18].

In our earlier paper [19], all the possible molecules which can be involved in the gas phase uncatalyzed CO_2 hydrogenation to methanol with a ratio of 4:1 (H_2:CO_2) have been investigated. A network of the hydrogenation process has been constructed by using computational tools [20], and the most favourable pathway leading to methanol and methane has been selected. Knowing that carbon dioxide can be absorbed by water as it happens in the oceans, we have envisaged and studied a water enhanced hydrogenation mechanism from a thermodynamic point of view. The mechanism has been compared energetically with the previously studied gas phase process.

2. Computational methods

A reaction network has been constructed and all the thermodynamic properties of the involved species and transition states at standard conditions have been computed by using the Gaussian 09 program package [21]. The Potential Energy Surface (PES) of the studied reaction has been analyzed and the important points (minima, TS, etc.) have been located. IRC (Internal Reaction Coordinates) [22] calculations have been used to verify that the transition states are located between the corresponding minima. Initially, the calculations have been carried out by using the B3LYP density functional theory (DFT) method [23,24] in combination with the 6-31G(d) basis set [25]. To further improve the accuracy of the analysis, the structures have been recalculated by using the W1U (Unrestricted Weizmann-1) composite method [26–28]. To mimic the solvent effects of bulk water, the calculations have been carried out by using the conductor-like polarizable continuum model, CPCM [29,30]. In our previous paper [19], W1BD [27] was applied for gas phase calculations, but it was not applicable in this case, because the BD algorithm is not compatible with the applied CPCM solvation model [29,30], and thus, the W1U method has been selected instead. The two methods were compared in gas phase calculations and gave almost identical results with less than 1 kJ/mol deviation (Table S1).

To estimate the accuracy of the level of theory used in this case (W1U), we carried out calculations for the elementary reaction steps and computed the reaction enthalpies of a simple mechanism which is close to our system (converts CO_2 and hydrogen to methanol and methane, Fig. 1) and can be compared to experimental values by using the heat of formations of the species available in the literature [31].

The envisaged test reaction includes successive H_2 addition steps, where the formic acid, formaldehyde and methanol are formed, leading to the formation of methane (Fig. 1). The computed enthalpy changes of each molecule produced through the elementary reactions and their respective experimental gas phase enthalpy of formation differences are listed in Table 1.

The highest absolute deviation between the computed and the

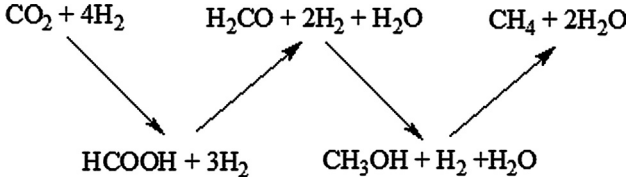

Fig. 1. Reaction steps of CO_2 hydrogenation to methane.

Table 1
Comparison of the computed enthalpy changes (ΔH°_r) of each molecule produced through elementary reaction steps and their respective experimental gas phase enthalpy of formation ($\Delta\Delta_f H_{exp}$) differences. The calculated and experimental values have also been compared and listed in the table (Calc-Exp).

	ΔH°_r (kJ/mol)	$\Delta\Delta_f H_{exp}$ (kJ/mol)	|Calc-Exp| (kJ/mol)
	Calc	Exp	
CO_2 + $4H_2$	0.00	0.00	0.00
HCOOH + $3H_2$	13.93	14.91	0.98
H_2CO + $2H_2$ + H_2O	40.08	35.78	4.30
H_3COH + H_2 + H_2O	−53.78	−49.81	3.97
CH_4 + 2 H_2O	−169.16	−165.02	4.14

experimental values belongs to (H_2CO + $2H_2$ + H_2O) which is equal to 4.30 kJ/mol. All in all, it can be considered that our computed results are precise. The experimental values of the species as well as their respective computed values are listed in the supporting information (Table S2).

3. Results and discussion

A newly designed CO_2 – methanol conversion mechanism is presented here, which involves several intermediates and transition states and applies $3H_2$, H_2O and H_3O^+ as additional reactants. CO_2 + $3H_2$ + H_2O + H_3O^+ was selected as a reference to compute the relative thermodynamic properties of the individual steps (*e.g.* $\Delta G^o_r = G_{(X)} - G_{ref}$, where $G_{(X)}$ and G_{ref} are the Gibbs free energy of structure X and the reference species, respectively).

The reaction pathways leading to methanol are starting either with a hydration or a protonation step (Fig. 2).

As a first step CO_2 (**A**) can be either hydrated to form carbonic acid (**B**), or protonated (**J**). The centre element of the mechanism is the protonation of formic acid (**DE**). To reach this point, four alternative pathways can be followed:

a) **ABCDE route** (blue): by the hydration of CO_2 (**A**) carbonic acid (**B**) will form (there are three conformations, the one considered here is higher in energy by 3.14 kJ/mol than the most stable conformation). This will be hydrogenated to reach methanetriol (**C**) which could reach formic acid (**D**) by a water elimination ($\mathbf{TS_{CD}}$). Then, formic acid can be protonated to form (**E**).
b) **ABLE route** (red): **(L)** can be achieved by the protonation of carbonic acid (**B**) which is the product of the CO_2 hydration. The hydrogenation of **(L)** will lead directly through ($\mathbf{TS_{LE}}$) to the protonated formic acid **(E)** and the formation of an extra water molecule.
c) **AJE route** (pink): The protonation of CO_2 followed by a hydrogenation ($\mathbf{TS_{JE}}$) leads directly to the protonated formic acid **(E)** through only two elementary steps.
d) **AJKLE route** (green): In this route additional elementary steps and one intermediate molecule links the *red* and the *pink* routes mentioned above. The molecule (**K**) is a protonated carbonic acid, which can be formed by a hydration of the protonated carbon dioxide (**JK**) or by the protonation of carbonic acid (**BK**). Then, a hydrogen shift could occur ($\mathbf{TS_{KL}}$) to produce (**L**).

Then, the protonated formic acid (**E**) is hydrogenated to form (**F**), from where a water elimination will lead to (**G**), which is a protonated formaldehyde. After this point, another hydrogenation ($\mathbf{TS_{GH}}$) will occur to reach the protonated methanol (**H**) and the final step will be the release of the proton to a water molecule forming methanol (**I**) and hydronium ion. The thermodynamic properties of the pathways have been computed (Table 1) and compared (Fig. 2).

The Fig. 3 can be divided into two parts: **[A-E]** and **[E-I]**. In the case of **[A-E]** the conversion of CO_2 (**A**) to protonated formic acid (**E**)

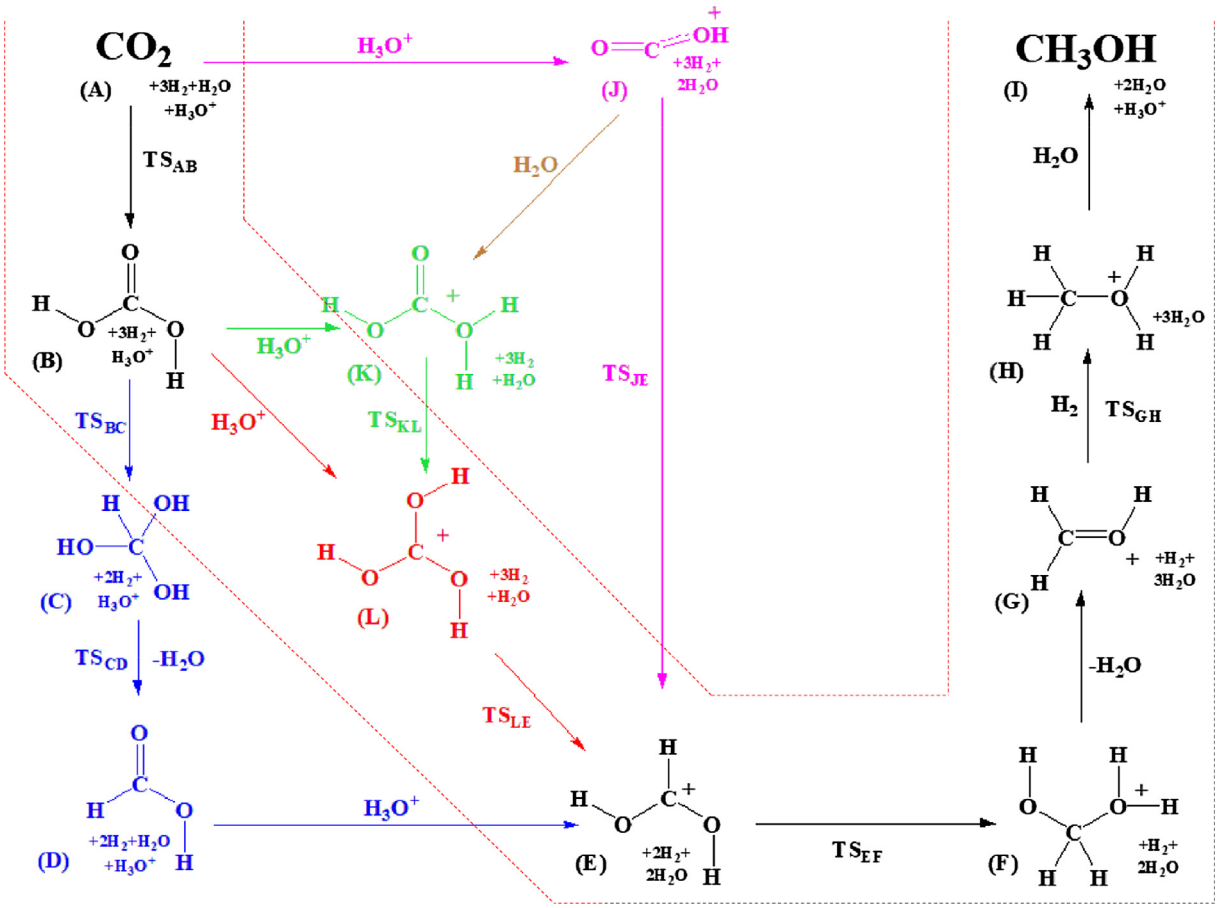

Fig. 2. Reaction pathways of the envisaged water enhanced CO_2 – methanol conversion. Letters are assigned to every structure, and each transition state is named as TS followed respectively with the letter referring to the reactant and then the product (*e.g.* TS_{AB}). The preferred pathway is highlighted by dashed lines.

occurs through several different pathways, while **[E-I]** is one single route where (**E**) will be converted to methanol (**I**) after 4 consecutive reaction steps.

In the **[A-E]** part of the mechanism, all the routes starts with a hydration of CO_2 (**A**) to carbonic acid (**B**), except for the *pink* pathway which goes directly from CO_2 (**A**) through a protonation followed by a hydrogenation to the protonated formic acid (**E**) with one single barrier ($\Delta G^{o}_{TS\_JE}$ = 383.18 kJ/mol) which is the second highest energy barrier in the system. The *blue* pathway shows the possibility to reach (**E**) through three reaction steps, within which there are two transition states (TS) and one of which ($\mathbf{TS_{BC}}$) corresponds to the highest barrier height in the system with a value of 402.34 kJ/mol. The other two steps are ($\mathbf{TS_{CD}}$, $\Delta G^{o}_{TS\_CD}$ = 255.58 kJ/mol) and (**DE**) which is a barrierless reaction step. Through the *red* pathway, the protonated formic acid (**E**) can be reached from the carbonic acid with only two reaction steps where one is a barrierless process (**BL**) while the other is a hydrogenation ($\Delta G^{o}_{TS\_LE}$ = 355.52 kJ/mol) which is the lowest hydrogenation energy barrier in the **[A-E]** section, and this makes it the preferred pathway. The overall preferred pathway would be then: **[A-TS_{AB}-B-BL-L-TS_{LE}-E-TS_{EF}-F-G-TS_{GH}-H-HI-I]** .

It is possible to link the *pink* and *red* pathway through the hydration reaction (**JK**) highlighted with the frame (*, Fig. 3), followed by the hydrogen shift ($\Delta G^{o}_{TS\_KL}$ = 256.78 kJ/mol) which is a part of the *green* reaction channel.

The two highlighted steps (**JK**) (*) and (**HI**) (**) are representing the two types of barrierless reactions (Morse potential) in the system (Fig. 3). All the possible pathways involve protonation steps. It is important to note that, in these cases, the reaction is barrierless and goes through a minimum instead of a transition state, and these are double Morse potentials (association + dissociation). (**HI**) (**, Fig. 4) was used as an example to describe these cases (**AJ, BK, BL, DE** and **HI**). The second type of barrierless step is a simple Morse potential reaction of a (de)hydration, where (**JK**) (*, Fig. 3) was used as an example.

The relative total energy change of the reaction (**HI**) (Fig. 4, left) has a shape of a parabola with a plateau at each extremity. The beginning of the reaction is at the first plateau, where the water molecule and the protonated methanol form a complex (protonated methanol-water). After this point, the total energy decreases and reach a minimum (first Morse potential), where the proton belongs to both methanol and water. Then, the energy increases to advance to another plateau (second Morse potential), where the products are located. Thus, the product is formed (methanol + H_3O^+) without going through an energy barrier.

In case of (**JK**) (Fig. 4, right), the total energy decreases from the reactant energy level ($H_3COH_2^+ + H_2O$) directly to the energy level of the products (H_3COH + H_3O^+) without going through an energy barrier.

Since the barrierless reaction (**DE**) is the second energetically lowest reaction of the system, it has also been studied through a flexible scan (Fig. 5).

The reaction (**DE**) is a barrierless process, which is similar to (**HI**) discussed above. The reaction decreases to a local minimum where the total energy change is close to 0 kJ/mol, as well as the relative Gibbs energy (see ΔG_{DE} at the Table 2). At this point, the protonated formic acid is forming a molecular complex with a water molecule, and the energy increases with the increasing distance between the water molecule and the protonated formic acid. The red dashed part of the graphic represents an internal conformational change, the oxygen atom of the water molecule got an interaction with the second closest hydrogen from the protonated formic acid while the distance between the

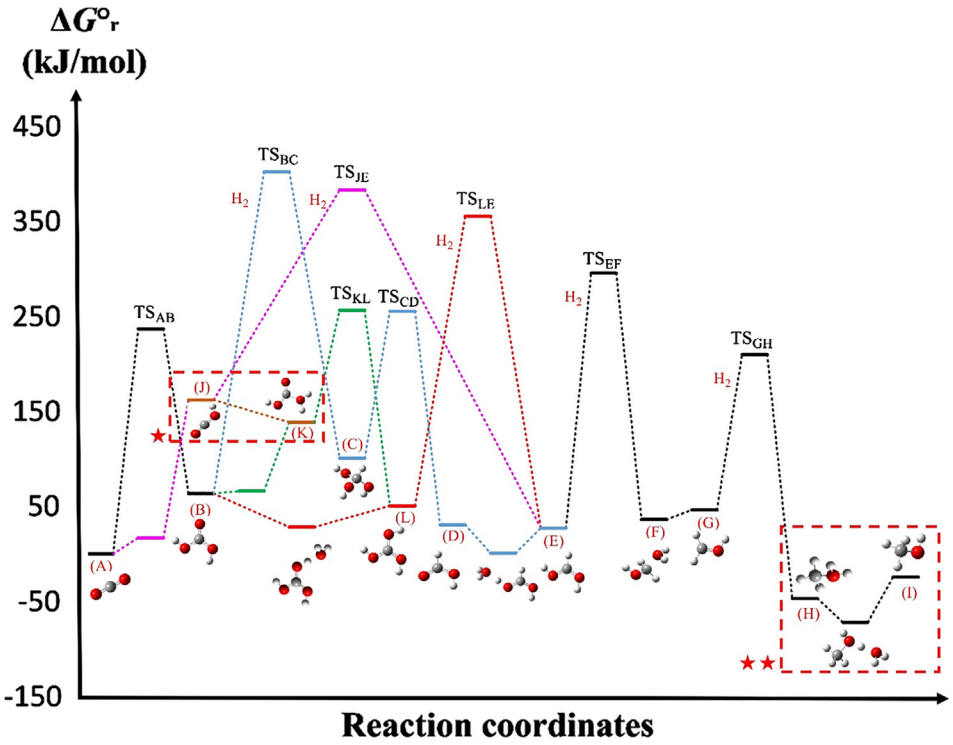

Fig. 3. Gibbs free energy change (ΔG_r^o, kJ/mol) of the water enhanced conversion of CO_2 to methanol calculated at the W1U level of theory. The transition states are named as TS followed by the reactant and the product, where the hydrogenation steps are highlighted with the (H_2) sign close to the barrier. (**B**), (**K**), (**E**) and (**L**) could have more than one conformer. *Morse potential of the barrierless elementary reaction step **JK**. **Double Morse potential of the barrierless elementary reaction step **HI**.

two molecules was increasing during the flexible scan.

The highest energy barriers of the pathways are $\Delta G^o_{TS\_BC}$ = 402.34 kJ/mol, $\Delta G^o_{TS\_JE}$ = 383.18 kJ/mol, $\Delta G^o_{TS\_LE}$ = 355.52 kJ/mol and $\Delta G^o_{TS\_EF}$ = 295.83 kJ/mol (Table 1), and all of the corresponding reaction steps are hydrogenations (H_2 molecule addition). Surprisingly, the last hydrogenation reaction step ($\Delta G^o_{TS\_GH}$ = 209.81 kJ/mol) is in the range and even lower, than the other processes such as hydrations (*e.g.* $\Delta G^o_{TS\_AB}$ = 237.28 kJ/mol), dehydrations (*e.g.* $\Delta G^o_{TS\_CD}$ = 255.58 kJ/mol) and hydrogen shifts (*e.g.* $\Delta G^o_{TS\_KL}$ = 256.78 kJ/mol).

Exothermic reactions are necessary to be involved in energy storage applications, ($\Delta H^\circ_r < 0$). Although the relative enthalpy values of $HCOOH_2^+$, $H_2O\text{-}H_2COH^+$ and $H_3COH_2^+$ is negative (Table 2), these products are non-isolable, and thus, the only remaining option for energy storage will be methanol (ΔH^o_{H3COH} = -77.06 kJ/mol in the studied mechanism. Comparing this value to the amount of heat of the highest energy barrier (ΔH_{TS_LE} = 284.66 kJ/mol) allow us to determine the theoretical efficiency of methanol formation in the mechanism. It corresponds to the ratio of the stored enthalpy $|\Delta H_r^o|$ and the invested enthalpy (the highest activation energy of the reaction path ΔH_{TS}^{max}).

$$\eta = \frac{|\Delta H_r^o|}{\Delta H_{TS}^{max}} = \frac{|\Delta H^o_{H3COH}|}{\Delta H_{TS\_LE}} \quad (2)$$

From our previous work [19], storing energy in methanol through the gas phase uncatalyzed mechanism would be done with an efficiency ofη = 14.4%, while in the current case, η = 27.1%, which is almost two

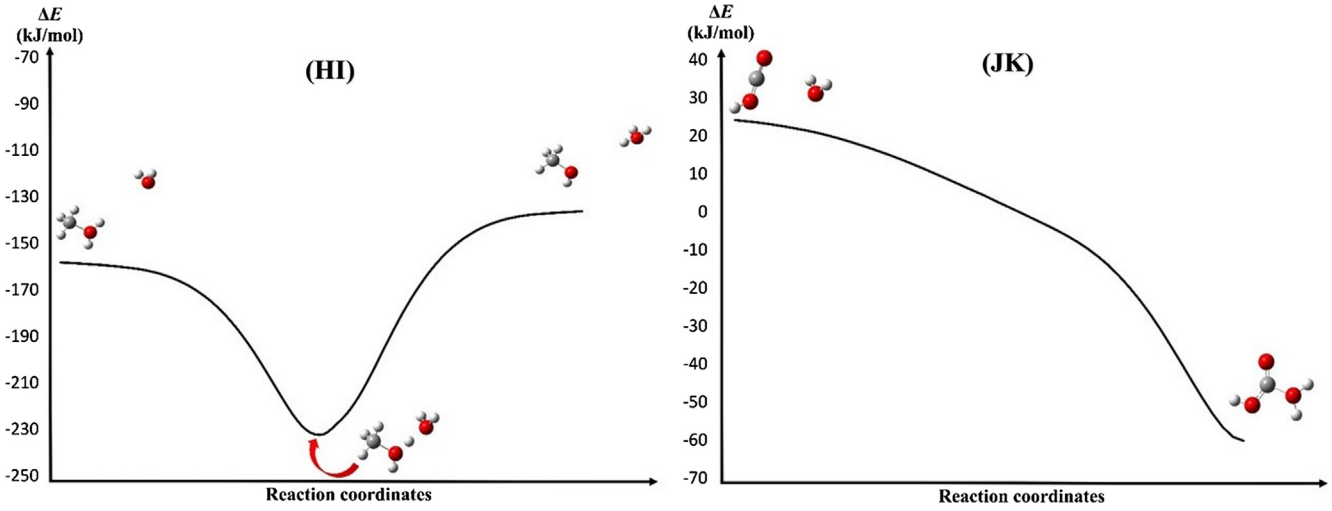

Fig. 4. Total energy change (ΔE_{tot}) of the two types of barrierless reactions (**JK**) (Morse potential, hydration) and (**HI**) (Double Morse potential, protonation).

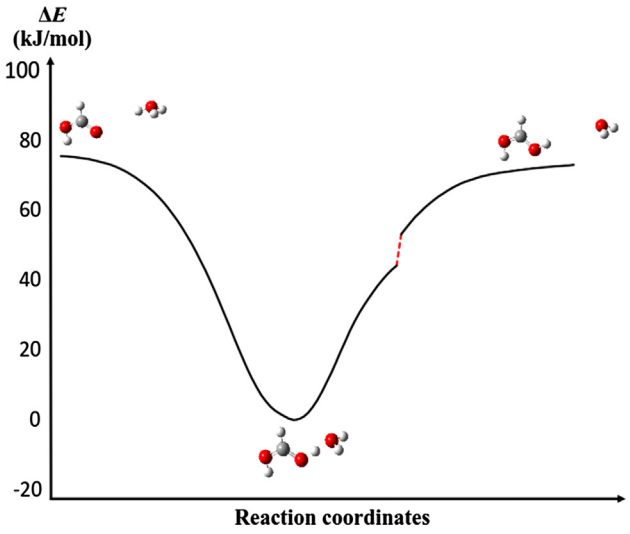

Fig. 5. Total energy change (ΔE_{tot}) of the (**DE**) reaction step (double Morse potential).

Table 2
Thermodynamic properties (ΔH^{o}_{r}, ΔG^{o}_{r} in kJ/mol and S in J/mol*K) of the studied carbon dioxide – methanol conversion reaction mechanism have been calculated at the W1U level of theory. The transition states of each elementary reaction steps are named as TS followed with the letter of the reactant and then the product (*e.g.* **TS_{AB}**). The barrierless reactions are noted by giving a letter of the reactant followed by the product (*e.g.* **AJ**). The most important structures of the preferred pathway are highlighted in red.

Code	Particules	$\Delta H^{\circ}{}_{r}$	$\Delta G^{\circ}{}_{r}$	S
		kJ / mol		J / mol K
A	CO_2	0.00	0.00	213.78
B	H_2CO_3	23.96	63.41	270.16
C	$HC(OH)_3$	28.15	100.93	288.63
D	HCOOH	2.30	30.80	248.48
E	$HCOOH_2^+$	-4.47	27.38	250.68
F	H_2O-H_2COH^+	-28.17	36.42	271.12
G	H_2COH^+	25.23	46.46	227.86
H	$H_3COH_2^+$	-101.81	-46.78	244.74
I	H_3COH	-77.06	-24.24	238.71
J	HCO_2^+	166.11	162.31	239.96
K	$H_3CO_3^+$	98.83	138.67	282.28
L	$C(OH)_3^+$	7.97	50.75	272.44
TS_{AB}	A → B	270.25	237.28	270.25
TS_{BC}	B → C	282.42	402.34	282.42
TS_{CD}	C → D	282.31	255.58	282.31
TS_{EF}	E → F	263.21	295.83	263.21
TS_{GH}	G → H	238.87	209.81	238.87
TS_{JE}	J → E	256.89	383.18	256.89
TS_{KL}	K → L	271.27	256.78	271.27
TS_{LE}	L → E	284.66	355.52	284.66
AJ	A-H_3O^+	-13.29	17.08	314.03
BK	B-H_3O^+	-9.17	65.54	354.05
BL	B-H_3O^+	-49.12	28.49	344.31
DE	D-H_3O^+	-66.50	0.97	319.88
HI	H-H_2O	-163.16	-71.79	311.58

times higher.

The two preferred pathways of CO_2 conversion to methanol in gas phase and aqueous phase have been compared (Table 3). It has to be emphasized that the aqueous phase pathway involves some ionic and barrierless reactions, while the gas phase pathway doesn't. In the best aqueous phase pathway, there is only one energy barrier higher than

Table 3
The comparison of the preferred carbon dioxide-methanol conversion pathways in gas and aqueous phase.

	Gas phase [19]	Aqueous phase
Barrierless reactions	No	Yes
Ionic reactions	No	Yes
Number of barriers > 300 kJ/mol	All (4)	Only one
Highest energy barrier (kJ/mol)	400.66	355.52
Efficiency (η)	14.4%	27.1%

300 kJ/mol $\Delta G^{o}_{TS\_LE}$ = 355.52 kJ/mol, unlike in the case of gas phase, all the barriers are > 300 kJ/mol. The rate of the recovered energy from what has to be invested in the uncatalyzed methanol formation from CO_2 hydrogenation in gas phase and aqueous phase has also been provided, and in the case of the aqueous phase mechanism the efficiency is 27.1%, which is almost two times higher than in the gas phase.

4. Conclusion

The conversion of CO_2 to methanol is a rather complicated multi-step process. A newly developed mechanism has been envisaged and studied. The pathways included into the mechanism can be divided into two categories, one of them involves the hydrogenation of a double bond and the other involves either water addition or subtraction, hydrogen shift or protonation. The former steps require high, while the latter require moderate activation energy.

The best pathway for the CO_2 - methanol conversion in aqueous phase involves 8 intermediates, 7 reaction steps, where 4 have a transition state and 3 are barrierless. The highest energy barrier ($\Delta G^{o}_{TS\_LE}$ = 355.52 kJ/mol) corresponds to (**TS_{LE}**) which is a hydrogenation. The energy storage is possible only through an exothermic reaction, and the only stable possible product of the proposed system is methanol which gives an efficiency equal to η = 27.1% in aqueous phase, which is almost two times better than the previously studied gas phase mechanism (η = 14.4%). By understanding the mechanism, special purpose catalysts can be designed to decrease the energy barrier and increasing the efficiency of the reaction.

CRediT authorship contribution statement

Rachid Hadjadj: Investigation, Data curation, Formal analysis, Visualization, Writing - original draft. **Imre G. Csizmadia:** Validation, Conceptualization. **Péter Mizsey:** Conceptualization, Methodology. **Svend Knak Jensen:** Resources, Conceptualization. **Béla Viskolcz:** Conceptualization, Supervision, Funding acquisition. **Béla Fiser:** Conceptualization, Project administration, Writing - review & editing.

Declaration of Competing Interest

The authors declare that they have no known competing financial interests or personal relationships that could have appeared to influence the work reported in this paper.

Acknowledgments

This research was supported by the European Union and the Hungarian State, co-financed by the European Regional Development Fund in the framework of the GINOP-2.3.4-15-2016-00004 project, aimed to promote the cooperation between the higher education and the industry.

Appendix A. Supplementary material

Supplementary data to this article can be found online at https://doi.org/10.1016/j.cplett.2020.137298.

References

[1] D.H. Vo, H.M. Nguyen, A.T. Vo, M. McAleer, CO2 Emissions, energy consumption and economic growth, Econom. Inst. Res. Pap., no. EI2019-11, Mar. 2019.
[2] W. Chandler, Energy and Environment in the Transition Economies, Routledge, 2018.
[3] J.-P. Gattuso, L. Hansson, Ocean acidification, Oxford University Press, 2011.
[4] P. Larkin, W. Leiss, D. Krewski, Risk assessment and management frameworks for carbon capture and geological storage: A global perspective, Int. J. Risk Assess. Manag. 22 (3–4) (2019) 254–285.
[5] E.E. Adams, K. Caldeira, Ocean storage of CO_2, Elements 4 (5) (Oct. 2008) 319–324.
[6] M.T. Islam, N. Huda, A.B. Abdullah, R. Saidur, A comprehensive review of state-of-the-art concentrating solar power (CSP) technologies: Current status and research trends, Renew. Sustain. Energy Rev. 91 (2018) 987–1018.
[7] J. Banerjee, K. Dutta, D. Rana, Carbon Nanomaterials in Renewable Energy Production and Storage Applications, Springer, Cham, 2019, pp. 51–104.
[8] S. Weitemeyer, D. Kleinhans, T. Vogt, C. Agert, Integration of Renewable Energy Sources in future power systems: The role of storage, Renew. Energy 75 (2015) 14–20.
[9] G. Leonzio, State of art and perspectives about the production of methanol, dimethyl ether and syngas by carbon dioxide hydrogenation, J. CO2 Util. 27 (2018) 326–354.
[10] X.-M. Hu, K. Daasbjerg, Carbon dioxide efficiently converted to methanol, Nature 575 (2019) 598–599.
[11] C. Steinlechner, H. Junge, Renewable methane generation from carbon dioxide and sunlight, Angew. Chemie Int. Ed. 57 (1) (Jan. 2018) 44–45.
[12] G.A. Olah, A. Goeppert, G.K.S. Prakash, Beyond oil and gas: the methanol economy, vol. 2006, no. 10. WILEY-VCH, 2006.
[13] A.J. Pain, J.B. Martin, C.R. Young, Sources and sinks of CO_2 and CH_4 in siliciclastic subterranean estuaries, Limnol. Oceanogr. (2019).
[14] A. Xia, X. Zhu, Q. Liao, Hydrogen Production from Biological Sources, Fuel Cells and Hydrogen Production, Springer New York, New York, NY, 2019, pp. 833–863.
[15] G. Centi, E.A. Quadrelli, S. Perathoner, Catalysis for CO_2 conversion: a key technology for rapid introduction of renewable energy in the value chain of chemical industries, Energy Environ. Sci. 6 (6) (2013) 1711.
[16] F. Samimi, N. Hamedi, M.R. Rahimpour, Green methanol production process from indirect CO_2 conversion: RWGS reactor versus RWGS membrane reactor, J. Environ. Chem. Eng. 7 (1) (2019) 102813.
[17] D. Sheldon, Methanol production – A technical history, Johnson Matthey Technol. Rev. 61 (3) (2017) 172–182.
[18] M. Huš, V.D.B.C. Dasireddy, N. Strah Štefančič, B. Likozar, Mechanism, kinetics and thermodynamics of carbon dioxide hydrogenation to methanol on $Cu/ZnAl_2O_4$ spinel-type heterogeneous catalysts, Appl. Catal. B Environ. 207 (2017) 267–278.
[19] R. Hadjadj, C. Deák, Á.B. Palotás, P. Mizsey, B. Viskolcz, Renewable energy and raw materials – The thermodynamic support, J. Clean. Prod. 241 (2019) 118221.
[20] A.J.C. Varandas, Straightening the hierarchical staircase for basis set extrapolations: a low-cost approach to high-accuracy computational chemistry, Annu. Rev. Phys. Chem. 69 (1) (Apr. 2018) 177–203.
[21] M.J. Frisch, G.W. Trucks, H.B. Schlegel, G.E. Scuseria, M.A. Robb, J.R. Cheeseman, G. Scalmani, V. Barone, G.A. Petersson, H. Nakatsuji, X. Li, M. Caricato, A. Marenich, J. Bloino, B.G. Janesko, R. Gomperts, B. Mennucci, H.P. Hratchian, J.V. Ortiz, A.F. Izmaylov, J.L. Sonnenberg, D. Williams-Young, F. Ding, F. Lipparini, F. Egidi, J. Goings, B. Peng, A. Petrone, T. Henderson, D. Ranasinghe, V.G. Zakrzewski, J. Gao, N. Rega, G. Zheng, W. Liang, M. Hada, M. Ehara, K. Toyota, R. Fukuda, J. Hasegawa, M. Ishida, T. Nakajima, Y. Honda, O. Kitao, H. Nakai, T. Vreven, K. Throssell, J.A. Montgomery, Jr., J.E. Peralta, F. Ogliaro, M. Bearpark, J. J. Heyd, E. Brothers, K.N. Kudin, V.N. Staroverov, T. Keith, R. Kobayashi, J. Normand, K. Raghavachari, A. Rendell, J.C. Burant, S.S. Iyengar, J. Tomasi, M. Cossi, J.M. Millam, M. Klene, C. Adamo, R. Cammi, J.W. Ochterski, R.L. Martin, K. Morokuma, O. Farkas, J.B. Foresman, D.J. Fox, Gaussian 09, Revision E.01, Gaussian Inc. 2013.
[22] L. Deng, T. Ziegler, L. Fan, A combined density functional and intrinsic reaction coordinate study on the ground state energy surface of H_2CO, J. Chem. Phys. 99 (5) (1993) 3823–3835.
[23] K. Kim, K.D. Jordan, Comparison of density functional and MP2 calculations on the water monomer and dimer, J. Phys. Chem. 98 (40) (1994) 10089–10094.
[24] P.J. Stephens, F.J. Devlin, C.F. Chabalowski, M.J. Frisch, Ab initio calculation of vibrational absorption and circular dichroism spectra using density functional force fields, J. Phys. Chem. 98 (45) (1994) 11623–11627.
[25] R. Ditchfield, W.J. Hehre, J.A. Pople, Self-consistent molecular-orbital methods. IX. An extended Gaussian-type basis for molecular-orbital studies of organic molecules, J. Chem. Phys. 54 (2) (1971) 724–728.
[26] S. Parthiban, J.M.L. Martin, Assessment of W1 and W2 theories for the computation of electron affinities, ionization potentials, heats of formation, and proton affinities, J. Chem. Phys. 114 (14) (2001) 6014–6029.
[27] E.C. Barnes, G.A. Petersson, J.A. Montgomery, M.J. Frisch, J.M.L. Martin, Unrestricted coupled cluster and Brueckner doubles variations of W1 theory, J. Chem. Theory Comput. 5 (10) (2009) 2687–2693.
[28] J.M.L. Martin, G. de Oliveira, Towards standard methods for benchmark quality ab initio thermochemistry—W1 and W2 theory, J. Chem. Phys. 111 (5) (1999) 1843.
[29] M. Cossi, N. Rega, G. Scalmani, V. Barone, Energies, structures, and electronic properties of molecules in solution with the C-PCM solvation model, J. Comput. Chem. 24 (6) (2003) 669–681.
[30] V. Barone, M. Cossi, Quantum calculation of molecular energies and energy gradients in solution by a conductor solvent model, J. Phys. Chem. A 102 (11) (1998) 1995–2001.
[31] E.W. Lemmon, M.O. McLinden, D.G. Friend, NIST Chemistry WebBook, NIST Standard Reference Database, no. 69, 2017.